Shape imperfections of reinforced concrete shell roofs

B. Elferink, P. Eigenraam, P.C.J. Hoogenboom, J.G. Rots

Delft University of Technology, the Netherlands

The precise geometries of three reinforced concrete shell roofs have been measured with a laser scanner. The resulting point cloud has been modelled by NURBS surfaces. Two methods have been developed for determining the shape imperfections with lengths between 0.5 and 5.5 m. The largest observed imperfection amplitude is 80 mm with a length of 5 m. The imperfections are represented by a variance spectrum and a normal distribution. A formula for the characteristic imperfection amplitude and the partial safety factor are derived.

Key words: Shell structures, geometrical imperfections, laser scanner, normal distribution, characteristic imperfection, partial factors

1   Introduction

Buckling of shell structures is sensitive to very small shape imperfections. Therefore, imperfections are added to finite element models for accurate nonlinear analysis. Often, the selected imperfection is equal to one of the buckling shapes, which can be obtained with a linear buckling analysis of the perfect shell [1]. The amplitude of this imperfection shape is very important for the shell strength (Koiter's half-power law) [2]. Clearly, the imperfection amplitude depends on the tools and workmanship of the builders. It was always difficult to measure shape imperfections in concrete shells and therefore this was left to engineering judgement. However, with modern laser scanners, accurate measurements can be performed on a much larger scale than before. Using modern software the data can be processed to quantify shape imperfection lengths and amplitudes.

In the presented research project, three reinforced concrete shell roofs have been measured by a laser scanner. These shells are Deitingen petrol station (1968), Heimberg swimming pool (1978) and Heimberg tennis hall (1978), all located in Switzerland. They have been designed by Heinz Isler and built by Willi Bösiger AG. The concrete was cast in situ on a formwork that consisted of steel scaffolding, curved glulam beams (approximately 180 x 50

mm spaced 800 mm) and wood floor board (Deitingen) or wood floor board and woodwool cement slabs as lost shuttering (Heimberg) [3, 4].

An overview of imperfections in all types of shell structure can be found in reference 5. Many imperfection measurements of airplane fuselages and rockets have been performed, though the conceived data base of imperfections seems to have not materialised [6]. Also reinforced concrete cooling towers are measured regularly, for example in reference 7 a reinforced concrete cooling tower is analysed showing a maximum shape deviation of 210 mm. As far as the authors know, imperfection measurements of reinforced concrete shell roofs have not been published before.

2   Measurements

Several measuring methods have been considered for determining shape imperfections in large shell structures. Laser scanning appeared to be the best option by far in terms of accuracy, measuring time and ease of transportation of the equipment [8].

2.1   Scanner

A laser scanner by Faro Technologies has been used [9]. The machine sends out laser pulses via a rotating mirror. The pulses reflect back from the measured surface to a light sensitive sensor on the machine. The machine measures the time it takes for the pulse to return. Subsequently, it calculates the distance to the point on the surface. The Cartesian x, y, z coordinates of a measured point are also calculated and stored. The machine rotates slowly to scan it's surroundings (table 1).

Table 1. Specifications of the laser scanner

Faro Focus 3D X130	
range	0.6 – 130 m
measuring speed	976 000 points per second
ranging error	± 2 mm at 25 m range, depending on the scanning speed

2.2   Scanning and data processing

The measurements have been performed on 2, 3 and 4 January 2015 [8]. Shells at five locations have been scanned. Not all data were usable due to obstacles in the scan field. Approximately, four scans of each shell have been made. A scan took less than half an

hour. During the scanning, protection binoculars are not necessary, therefore, it was possible to scan the swimming pool during opening hours (fig. 1). The point clouds that were used in this study are available on internet.

heronjournal.nl/61-3/scans.zip
scan1.txt Deitingen petrol station North; scan2.txt Deitingen petrol station South; scan3.txt Heimberg swimming pool; scan4.txt, Heimberg tennis hall

The points can be exported to most CAD programs by the program Scene [9]. Shell parts directly above the scanner have been scanned with an excessive amount of points, therefore, redundant points can be removed by the program CloudCompare [10]. To this end also Matlab [11] has been used. If a shell is scanned from several positions the data sets can be merged using spherical markers visible in each set. The program Rhino 5.0 has been used for analysing the point cloud [12]. The number of points need to be less than 1 million to prevent overload on a normal PC. Points on lamps, cables, and other objects were removed by hand.

2.3 Buckling lengths

The largest buckling length of cylindrical shells can be calculated by $1.7\sqrt{rt}$, where r is the shell radius of curvature and t is the shell thickness. The formula can also be used to
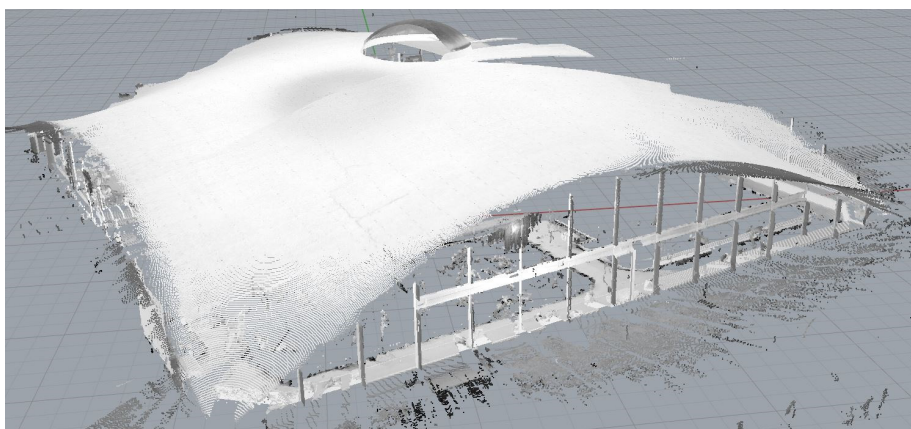
Figure 1. Point cloud of Heimberg swimming pool
The swimming pool has been scanned on the inside but the point cloud is observed from the outside.

estimate the buckling lengths of doubly curved shells [13]. The calculated buckling lengths are shown in table 2. The radii have been measured at the shell tops and the thicknesses have been obtained from literature [3, 4]. Buckling is particularly sensitive to imperfections with lengths that are approximately equal to the buckling length. In order to be rigorous, shape imperfections up to 6.0 m have been studied.

Table 2. Dimensions of the shell structures

	thickness	radius of curvature	buckling length
Deitingen petrol station	90 mm	25.2 m	2.6 m
Heimberg swimming pool	90	21.7	2.4
Heimberg tennis hall	95	25.0 short direction	2.6
		45.3 long direction	3.5

3   Surface fitting

A CAD program can fit a surface through a point cloud. The surface is a NURBS that is defined by control points. In the fitting process the control points are moved automatically in order to minimise the sum of all squares of the distances between the measured points and the surface. The more control points a NURBS surface has, the more accurately it can be fitted to the point cloud.

As a test, three artificial point clouds have been created with a length and width of 10 m. The coordinates of the points are described by $z = 50 \sin \frac{\pi x}{l} \sin \frac{\pi y}{l}$, where l is the half wave length. Three half wave lengths were considered, l = 500, 1000 and 1500 mm. The amplitude is 50 mm. NURBS surfaces with varying control point spacing have been fitted through these point clouds. The accuracy statistics – mean of the point distances to the surface – are plotted in figure 2. It can be observed that a NURBS surface with less than one control point per half-wave length cannot be fitted accurately, while a NURBS surface with more than one control points per half-wave length can be fitted accurately.

The conclusions is that a fitted NURBS surface does not describe an imperfection if the spacing between the control points is greater than the imperfection length. Based on this observation two methods were developed to quantify the shape imperfections. The *single surface method* and the *double surface method*.

mean point distance in mm

half-wave length of 0.5 m
half-wave length of 1.0 m
half-wave length of 1.5 m

number of control points per half-wave length
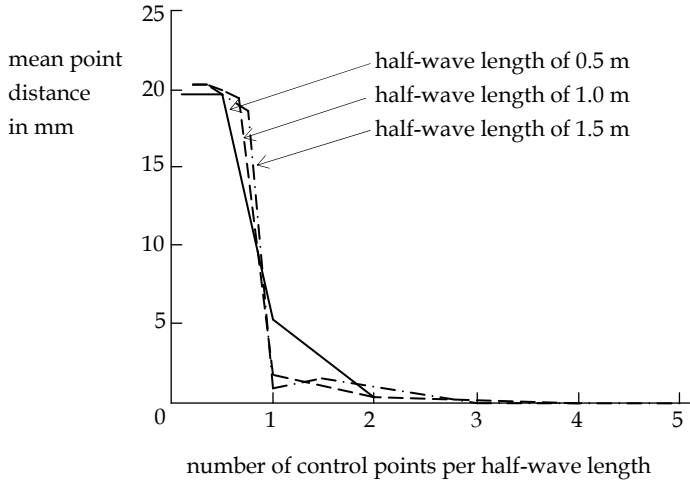
Figure 2. Accuracy of surface fitting for varying control point spacing

4   Single surface method

In the single surface method a surface is positioned between the point cloud. This surface is a square NURBS with evenly spaced control points. The surface is fitted to the point cloud. This is repeated with different distances between the control points. For each fit the mean distance and standard deviation of the distance of the points to the surface were determined by Rhinoceros (table 3). The statistics of Rhinoceros do not distinguish between points above and below a NURBS. The distribution of the point distances typically looks like the right half of a normal distribution. However, in the present study we do need to make a distinction between points above (positive) and below (negative). Therefore, the half distribution is transformed to a full distribution. The details of this are explained below.

In table 3 the variation coefficients (standard deviation over mean) vary between 0.67 and 0.91; the average is 0.79. The half-normal probability density function has a variation coefficient of 0. 76. Several other density functions have been considered but none came as close as the half-normal probability density function, therefore, this function was selected.

$$P = \begin{cases} 0 & \text{for} \quad \zeta < 0 \\ \dfrac{2}{b\sqrt{\pi}} e^{-(\frac{\zeta}{b})^2} & \text{for} \quad \zeta \geq 0 \end{cases} \tag{1}$$

Its mean is $\mu = \dfrac{b}{\sqrt{\pi}}$ and the standard deviation is $b\sqrt{\dfrac{\pi-2}{2\pi}}$.

On average half the data points are above the NURBS surface and half the points are below. Therefore, a sign can be assigned to the distances, obtaining the normal probability density function.

$$P = \frac{1}{b\sqrt{\pi}} e^{-(\frac{\zeta}{b})^2} \qquad -\infty < \zeta < \infty \tag{2}$$

Its mean is 0 and the standard deviation is $\dfrac{b}{\sqrt{2}}$.

Table 3. Fit results of the single surface method

control point spacing [m]	1.0	2.0	3.0	4.0	5.0	6.0
Deitingen petrol station North						
mean µ [mm]	2.51	5.11	7.31	9.46	13.16	20.61
standard deviation [mm]	2.03	3.72	5.62	7.57	8.91	15.25
Deitingen petrol station South						
mean µ [mm]	2.85	4.69	6.51	8.16	12.43	17.58
standard deviation [mm]	2.42	3.90	5.26	6.58	8.34	12.78
Heimberg swimming pool						
mean µ [mm]	1.94	3.40	4.15	4.81	5.36	5.67
standard deviation [mm]	1.66	2.69	3.42	4.03	4.87	5.17
Heimberg tennis hall						
mean µ [mm]	1.50	2.76	4.03	4.30	6.08	9.88
standard deviation [mm]	1.20	2.18	3.10	3.48	4.53	7.24

Variance is the square of the standard deviation. Therefore,

$$V = \frac{b^2}{2} = \frac{\pi}{2}\mu^2 \tag{3}$$

where V is the variance of the signed distances and µ is the mean of the distances computed by Rhinoceros. The results are shown in figure 3.

It is assumed that the signed distances d can be described as a stochastic field.

$$d = \sum a_i \sin(\frac{\pi x}{l_i} + \zeta_i)\sin(\frac{\pi y}{l_i} + \xi_i), \tag{4}$$

where a_i is an imperfection amplitude, l_i is an imperfection length and ζ_i, ξ_i are random phase shifts between 0 and 2π. The variance of this field is

$$V = \frac{1}{l^2} \int\limits_{x=0}^{l} \int\limits_{y=0}^{l} d^2 \, dx \, dy = \sum \frac{1}{4} a_i^2 \,, \tag{5}$$

where $l = \Pi \, l_i$. Consequently, variance can be decomposed in amplitudes of imperfection lengths.
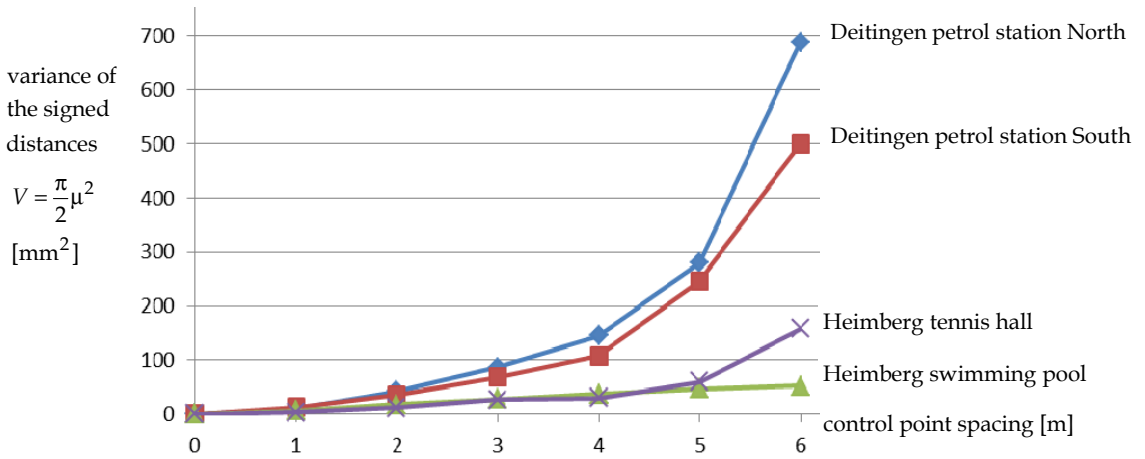
Figure 3. Fit results of the single surface method for the measured shells

Figure 3 shows the variance of all imperfections with a length smaller than 6 m; smaller than 5 m; smaller than 4 m, et cetera. Therefore, the variance of imperfections with lengths between, for example, 4 and 5 m can be obtained by subtraction. According to equation 5 the amplitude of the associated imperfections can be obtained with

$$a_i = \sqrt{4 \, \Delta V} \,. \tag{6}$$

The result is shown in table 4 and figure 4. It is observed that the Heimberg shells have been built more accurately than the Deitingen shells.[1] Figure 4 is a practical version of the variance spectra of stochastic fields. It may be used in stochastic finite element analyses.

---

[1] The Heimberg shells have an inner surface of woodwool cement slabs. The Deitingen shells have not. However, this is not the cause of the difference in imperfection amplitude. Woodwool cement slabs are still produced today. They have dimensions 0.6 × 1.3 m and a thickness tolerance of ± 4 mm.

Table 4. Imperfection amplitude a_i [mm] for several imperfection lengths l_i [m]

imperfection length [m]	0.0–1.0	1.0–2.0	2.0–3.0	3.0–4.0	4.0–5.0	5.0–6.0
Deitingen petrol station North	6.3	11.2	13.1	15.1	22.9	39.8
Deitingen petrol station South	7.1	9.3	11.3	12.3	23.2	31.4
Heimberg swimming pool	4.9	7.0	6.0	6.1	5.9	4.6
Heimberg tennis hall	3.8	5.8	7.4	3.8	10.8	19.5
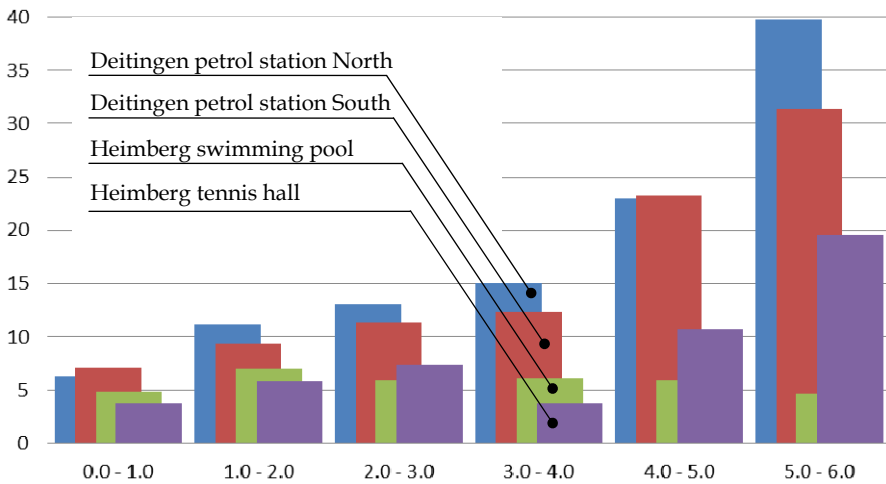
Figure 4. Imperfection amplitude a_i [mm] for several imperfection lengths l_i [m]

5   Double surface method

In the double surface method two surfaces are fitted through the point cloud. The first surface is a NURBS with control points spaced at 0.25 m. This surface can accurately match the shape including imperfections with half wave lengths of 0.25 m or longer. The second surface is a NURBS of the same size with control points spaced at a much larger distance, for example 3.00 m. This surface describes the shape of a shell without imperfections. The second control spacing should be much smaller than the shell dimensions, otherwise the shape of the shell would be distorted. If possible, the second control point spacing should be somewhat larger than the buckling length because imperfections of that length have the most influence on the shell buckling behaviour.

5.1 Plot results

The distance between the two surfaces is plotted in figures 5 to 8. This is accomplished by projecting a grid of points at both NURBS surfaces in a direction mostly perpendicular to the surfaces. So, each grid point has two projected points. The distances between each of these projected points are the distances between the surfaces. In the contour plots the largest imperfection amplitude and the corresponding imperfection length can be observed. The results are summarised in table 5.
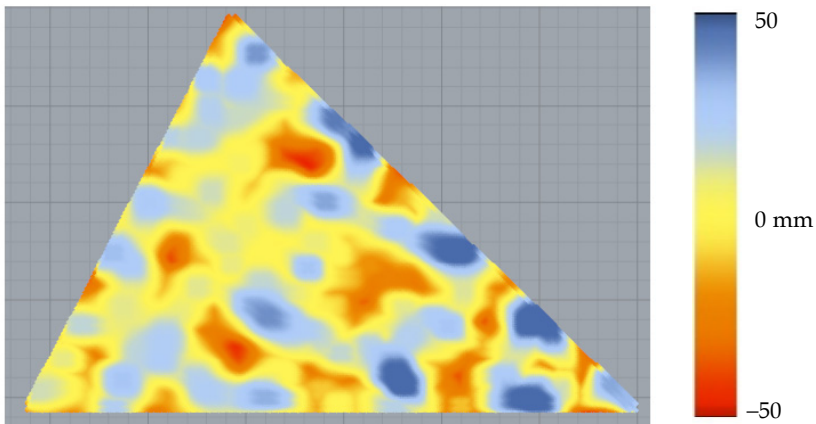
Figure 5. Shape imperfections in the North roof of Deitingen petrol station
Patch of 33 x 21 m; control point spacings of 0.25 and 4.70 m; largest observed imperfection
amplitude is 64 mm
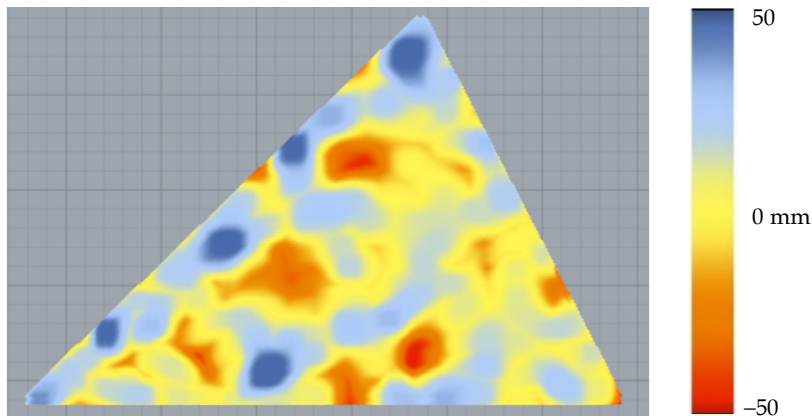
Figure 6. Shape imperfections in the South roof of Deitingen petrol station
Patch of 33 x 21 m; control point spacings of 0.25 and 4.70 m; largest observed imperfection
amplitude is 60 mm
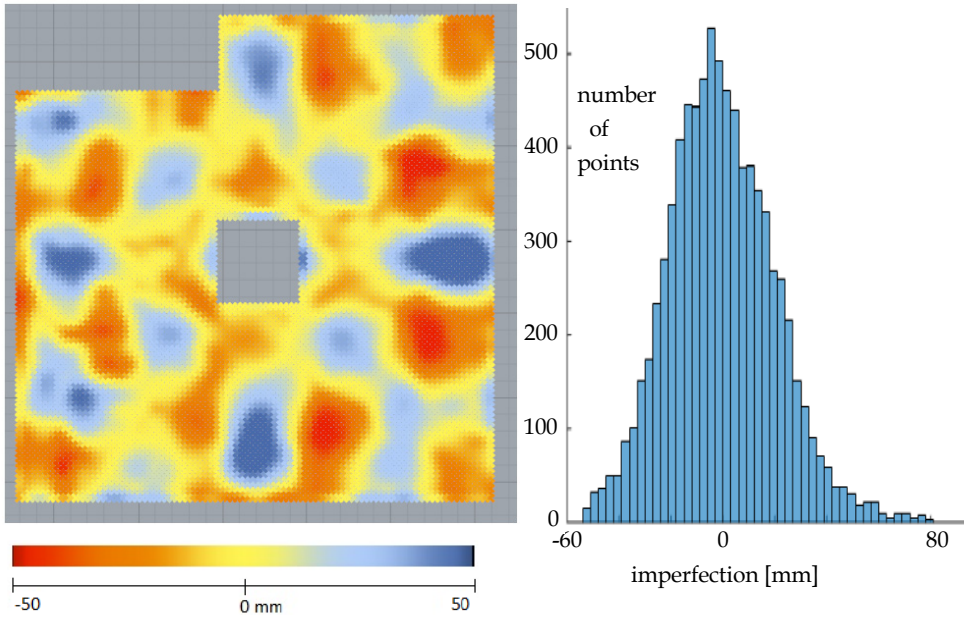
Figure 7. Shape imperfections in the roof of Heimberg swimming pool

Patch of 29 x 28 m; control point spacing of 0.25 and 5.00 m; largest observed imperfection
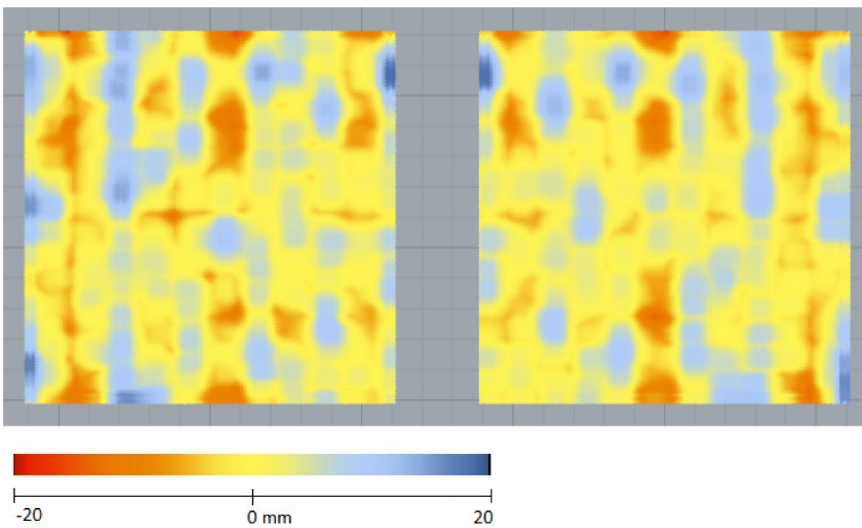
amplitude is 80 mm

Figure 8. Shape imperfections in the roof of Heimberg tennis hall

Two patches of 12 x 12 m; control point spacing of 0.25 and 4.00 m; largest observed imperfection

amplitude is 23 mm

186

The focus on the largest imperfection in a shell structure seems over-conservative. A structure does not need to fail at the location of the largest imperfection. As an example consider a brick wall with openings for doors and windows. It would be extremely coincidental if at the location of the smallest strength also the largest stress occurs. However, shells roofs are an exception. They are optimised to have approximately the same compressive stress everywhere. [2] If a perfect shell would be possible, it would have many buckling modes with corresponding buckling load factors that are almost the same. Therefore, shells buckle at the location of the largest imperfection. The place of this imperfection makes almost no difference.

Table 5. Largest observed imperfection amplitudes in the double surface method

	peak $\hat{d}$ [mm]	length l [m]	area [m²]
Deitingen petrol station North	64	4.70	346
Deitingen petrol station South	60	4.70	346
Heimberg swimming pool	80	5.00	727
Heimberg tennis hall	23	4.00	288

The Heimberg largest deviations have been transformed to an area of 346 m² and a length of 4.70 m by equation 11. For this area and length the largest deviations of the shells are 64, 60, 62.5 and 25.9 mm respectively.[3] The mean of the latter values is 53.1 mm and the standard deviation is 18.2 mm. Assuming a normal distribution, the 5% characteristic value of the largest imperfection is 53.1 + 2.68 × 18.2 = 101.9 mm. The factor 2.68 is used instead of 1.64 because only four measurements are available. This is a recommended procedure in design by testing based on an unknown standard deviation [14, table D1]. Note that the consequence of only four measurements is an increase of the standard deviation by a factor 2.68/1.64 = 1.63.

---

[2] The word "compressive stress" is not accurate here. It should be "buckling membrane force". However, defining the buckling membrane force would make the argument unclear. We leave this for another paper.

[3] Thus, the results of Section 5.1 depend on the results of Section 5.3. Also, the results of Section 5.3 depend on the results of Section 5.1. This can be considered circular reasoning. However, the results converge quickly to the present values, therefore, it does not pose a problem.

5.2 Partial factor

When designing a shell structure it is not practical to perform nonlinear probabilistic analyses. Therefore, safety factors need to be derived. Partial factors of material strengths and loads are calculated with the following formulas [14].

$$\gamma_R = \frac{1 - kV_R}{1 - \alpha_R \beta V_R} , \qquad (7)$$

$$\gamma_S = \frac{1 - \alpha_S \beta V_S}{1 - kV_S} , \qquad (8)$$

where k defines the characteristic value, α_R and α_S are the sensitivity factors of material strengths and loads, β is the reliability index, V_R and V_S are the variation coefficients of material strengths and loads respectively. These formulas are very accurate for independent normally distributed variables when the sensitivity factors are known.

Shape imperfections could be related to self-weight and to extreme weather, however, it seems realistic to assume that the imperfections and the loading are sufficiently independent. A normal distribution is realistic for self-weight, however, snow load is better represented by a Gumbel distribution. Moreover, the distribution function of the largest shape imperfection is simply unknown. As an approximation we choose normal distributions for all stochastic variables. In theory, sensitivity factors are the result of a probabilistic finite element analysis, which is rather impractical. Fortunately, sensitivity factors can be conservatively estimated.

Shape imperfections act as load on shell structures therefore the later of the two formulas is applied. In the following section, the 5% characteristic value of the imperfection amplitude is used. The associated value of k is –1.64. The recommended sensitivity factor for a dominant load is α_S = –0.70. In case the imperfections are not dominant α_S = –0.28 [14, table E3]. Shell structures tend to fail abruptly which surely leads to loss of live. Also it is not very expensive to build a thicker shell. Therefore, an annual failure probability of 10^{-5} or smaller is appropriate. The associated value of β is 4.3 [14, table E2]. The variation coefficient of the imperfection amplitude is standard deviation over mean 1.63 × 18.2/53.1 = 0.559. Consequently, the partial factor of the imperfection amplitude is

$$\gamma = \frac{1 + 0.70 \times 4.3 \times 0.559}{1 + 1.64 \times 0.559} = 1.40 . \qquad (9)$$

This large partial factor is partly caused by the factor 1.63 which accounts for the uncertainty of using only four measurements.

5.3   Characteristic imperfection

In the previous sections, a normal distribution is adopted for the largest imperfection amplitude. The distribution is determined for an imperfection length of l = 4.7 m and a shell area of A = 346 m². The characteristic value of 101.9 mm needs to be extrapolated to other values of l and A. In Figure 4 it can be observed that the imperfection amplitude is approximately linear in l. Therefore, a linear relation is assumed between the mean of the largest imperfection amplitude and l.

There are few measurements available for extrapolating the imperfection amplitude in A. Fortunately, probability theory gives a clue on how to extrapolate. The Gumbel distribution and the Fréchet distribution describe positive maxima and can be mathematically transformed to other shell areas [15]. Both distributions have very a different shape than the normal distribution and there is no reason to assume that they can describe the four measurements well. Therefore, this aspect of the distributions is not used. The only aspect that is used is how the characteristic value changes with A (fig. 9). We selected the Fréchet distribution because it does not have negative amplitudes and its coefficient of variation is not affected by the transformation.
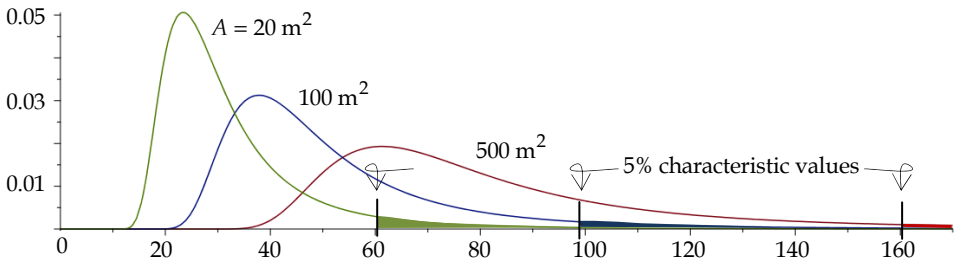
Figure 9. Fréchet distribution of the maximum imperfection amplitude for areas 20, 100 and 500 m²

The Fréchet distribution is

$$P(\hat{d} \leq \xi) = \exp(-\frac{u^b}{\xi^b}) \tag{10}$$

Its mean is $u\,\Gamma(1-\frac{1}{b})$ and the standard deviation is $\sqrt{u^2\,\Gamma(1-\frac{2}{b})-\text{mean}^2}$.

In the previous section it is shown that for an area of 346 m² the largest imperfection

amplitude has a mean of 53.1 mm and a standard deviation of 1.63 × 18.2 mm. These values are accurately produced by b = 3.3392 and u = 40.93 mm.

The mean imperfection amplitude is linear in the imperfection length l. For the measurements the imperfection length is 4700 mm. Therefore, it can be written that

$$u = 40.93 \text{ mm} = \frac{l}{114.8} \tag{11}$$

The Fréchet distribution has the property that the maximum of n maxima also has a Fréchet distribution. [4] For the new distribution the value b remains the same and the value of u becomes $u\sqrt[b]{n}$. Therefore, a shell with a surface area n times larger than the considered surface can be represented by

$$P(\hat{d} \le \xi) = \exp(-\frac{nu^b}{\xi^b}) . \tag{12}$$

The considered surface of 346 m² is 15.7 times the imperfection length squared.

$$n = \frac{A}{15.7 \, l^2} . \tag{13}$$

Substitution of equation 11 and 13 in 12 and rewriting gives

$$\xi = \frac{l}{114.8} (\frac{-A}{15.7 \, l^2 \ln(1-P)})^{\frac{1}{3.34}} \tag{14}$$

Assuming a characteristic value (P = 5%) the equation simplifies to

$$\xi = \frac{A^{0.3} l^{0.4}}{108} \tag{15}$$

As a check, the values of A = 346 m² and l = 4.7 m are substituted into the equation.

$$\xi = \frac{346^{0.3} \, 4.7^{\,0.4}}{108} = 0.0993 \text{ m} = 99.3 \text{ mm} , \tag{16}$$

which is almost the same as the characteristic value of 101.9 mm.

Equation 9 and 15 can be used in shell design. For example, consider a large reinforced concrete shell roof with a surface area of 1000 m². A finite element analysis shows that the

---

[4] A proviso is that the maxima are independent. In other words, the imperfections on the left hand side of a shell need to be independent of the imperfections in the right hand side, which we think is fulfilled on account of the construction process.

buckling length is 2 m. As an imperfection, the buckling shape is added to the finite element model with an amplitude of

$$\xi_c = \frac{1000^{0.3}\ 2^{0.4}}{108} = 0.097 \text{ m} = 97 \text{ mm}$$
$$\xi_d = 1.4\ \xi_c = 136 \text{ mm}$$

The authors do not think that Equations 9 and 15 are very accurate because they are based on only four scans. Nonetheless, Equation 15 includes all important parameters and the unit length is correctly represented. It is not unreasonable to expect that future measurements will show that this simple formula is useful, provided that the numbers 1.4, 0.3, 0.4 and 108 are somewhat adjusted.

6   Conclusions

- Modern laser scanners are very suitable for accurately measuring the shape of shell structures.
- A NURBS surface can be fitted through the measured data points. Shape imperfections with a length smaller than the control point spacing are not described by the NURBS surface.
- The statistics of surface fits for varying control point spacing can be used to determine the variance spectrum (Single surface method).
- The imperfections can be visualised as the distance between two surface fits. The first surface fit is accurate with a small control point spacing. The second surface fit is less accurate but still smooth with a control point spacing somewhat larger than the buckling length (Double surface method).
- The largest observed shape imperfection in the three reinforced concrete shell structures is 80 mm. This imperfection has a length of 5 m.
- The data has been used to determine a formula for the characteristic value of the shape imperfection amplitude. The formula depends on the imperfection length and the shell surface area, therefore, it includes a size effect. If buckling is the dominant failure mode then the partial factor for the imperfection amplitude is 1.40.

Literature

[1] Eurocode 3 - *Design of steel structures* - Part 1-6: Strength and stability of shell structures, CEN, Brussels, 2006

[2] W.T. Koiter, *Over de stabiliteit van het elastisch evenwicht*, dissertation, Delft University of Technology, 1945

[3] J. Chilton, *The engineer's contribution to contemporary architecture; Heinz Isler*, Thomas Telford Ltd, London, 2000, ISBN 0 7277 2878 4

[4] E. Ramm, E. Schunck, *Heinz Isler Schalen*, Hochsch.-Verl. an der ETH, Zurch, 2002, ISBN 3 7281 2792 2

[5] Imperfection sensitivity. L.A. Godoy, *Thin-walled structures with structural imperfections: Analysis and behavior*, Pergamon Press, Oxford, U.K., 1996, ISBN 0 08 042266 7

[6] J. Arbocz, Shell buckling research at Delft (1976-1996), report, Delft University of Technology

[7] C. Ioannidis, A. Valani, A. Georgopoulos, E. Tsiligiris, 3D model generation for deformation analysis using laser scanning data of a cooling tower, Proceedings of the *IAG/FIG Symposium*, Baden, May 22-24, 2006

[8] B. Elferink, Shell imperfections, A study of the shape and magnitude of geometrical imperfections in thin concrete shell structures , MSc report, *Delft University of Technology*, 2015

[9] Faro Technologies, online: faro.com, retrieved 08-01-2016

[10] CloudCompare, online: cloudcompare.org, retrieved 08-01-2016

[11] Matlab, online: www.mathworks.com, retrieved 02-02-2016

[12] Rhinoceros, online: rhino3d.com, retrieved 08-01-2016

[13] J. Blaauwendraad, J. Hoefakker, *Structural shell analysis, Understanding and application*, Springer, 2014, ISBN 9 400 76702 1

[14] ISO 2394, *General principles on reliability for structures*, International organization for standardization, Switzerland, 1998

[15] K. Bury, *Statistical distributions in engineering*, Cambridge University Press, Cambridge, 1999, ISBN 0 521 63232 3